Energy 315 (2025) 134275

Contents lists available at ScienceDirect

Energy

journal homepage: www.elsevier.com/locate/energy

Reducing environmental and human health impacts of energy systems through optimal utilization of transmission flexibilities

Eduardo J. Castillo Fatule [a,1], Yuanrui Sang [b,*,1], Jose F. Espiritu [c]

[a] Klipsch School of Electrical Engineering, New Mexico State University, Las Cruces, NM 88003, USA
[b] Department of Electrical and Computer Engineering, University of Massachusetts Amherst, Amherst, MA 01003, USA
[c] The Department of Mechanical and Industrial Engineering, Texas A&M University, Kingsville, TX 78363, USA

ARTICLE INFO

Handling editor: Isabel Soares

Index Terms:
Distributed flexible AC transmission systems (D-FACTS)
Environmental impacts
Evolutionary algorithm
Multi-objective optimization
Power system economics

ABSTRACT

Integrating renewable energy in power systems can significantly reduce emissions in the energy sector, resulting in remarkable environmental and human health benefits. One of the major barriers for renewable energy integration is transmission congestion, which can be effectively mitigated through optimal utilization of transmission flexibilities. Distributed flexible AC transmission systems (D-FACTS) are cutting-edge devices that can provide premium flexibility to electric power transmission systems when optimally allocated and configured. However, the optimal D-FACTS allocation and configuration problem is extremely computationally challenging. This study aims to present a computationally efficient algorithm that can optimally allocate and configure variable-impedance D-FACTS to minimize (1) power system operating costs, (2) global warming potential (GWP), and (3) human toxicity potential (HTP), considering uncertainties in load and renewable energy generation. The model was implemented on a modified RTS-96 test system with a high penetration of wind energy, and results show that optimally allocating and configuring D-FACTS can reduce power system operating costs, GWP, HTP, and renewable energy curtailment. The results also indicate an inverse relationship between the first objective and the other two, showing the necessity to choose a proper trade-off between cost savings, environmental and human health impacts.

Nomenclature

Indices	
a, b	Solutions
c	Contaminant
k	Transmission line.
g	Generator.
n	Node.
r	Renewable Generator.
s	Scenario.
seg	Segment of linearized generator cost function.
i	Objective or Fitness Function
Sets	
$\sigma^{+}(n)$	Transmission lines with their "to" bus connected to node n.
$\sigma^{-}(n)$	Transmission lines with their "from" bus connected to node n.
$g(n)$	Generators connected to node n.
$r(n)$	Renewable generators connected to node n.
Variables	
C^{D}_{inv}	Total investment in D-FACTS ($).

(*continued on next column*)

(*continued*)

$D_{a,b}$	Dominance of solution a over solution b
$F_{k,s}$	Real power flow through transmission line k in scenarios s.
$FM_{i,a}$	Value of fitness function i for solution a
$OF_{i,a}$	Value of objective function i for solution a
$P_{g,s}$	Real power generation of generator g in scenarios s.
$P^{C}_{r,s}$	Curtailed energy from renewable generator r in scenario s
$P^{seg}_{g,s}$	Real generation of generator g in scenarios s in segment seg.
$R^{D}_{g,s}$	Spinning down reserve available through generator g in scenario s.
$R^{U}_{g,s}$	Spinning up reserve available through generator g in scenario s.
x^{D}_{k}	Integer indicating the number of D-FACTS installed on transmission line k
$\theta_{b,s}$	Voltage angle at bus b in scenarios s.
$\theta_{fr,k,s}$	Voltage angle at the "from" node of line k in scenarios s.
$\theta_{to,k,s}$	Voltage angle at the "to" node of line k in scenarios s.
ϕ^{C}	Percentage of curtailed renewable energy.
Parameters	
C^{NL}_{g}	No load cost of generator g.
$C^{linear}_{g,seg}$	Linear cost of generator g in segment seg.

(*continued on next page*)

* Corresponding author.
E-mail addresses: ejcast@nmsu.edu (E.J. Castillo Fatule), ysang@umass.edu (Y. Sang), jose.espiritu@tamuk.edu (J.F. Espiritu).

[1] E. J. Castillo Fatule and Y. Sang's contributions to this work were supported by the U.S. National Science Foundation under Award #2131201.

https://doi.org/10.1016/j.energy.2024.134275
Received 5 August 2023; Received in revised form 10 December 2024; Accepted 23 December 2024
Available online 25 December 2024

(*continued*)

C_g^D	Down reserve cost of generator *g*.
C_g^U	Up reserve cost of generator *g*.
C_{single}^D	Cost a of single D-FACTS unit ($).
C_{sh}^D	Cost a of single D-FACTS unit converted to an hourly figure ($/h).
C_{inv}^{max}	Maximum investment allowed for D-FACTS.
$f_{k,s}$	Flow direction for line *k* in scenario *s*
F_k^{max}	Thermal capacity/voltage drop limit of transmission line *k*.
$G_{g,c}$	Gaseous contaminant *c* released by generator *g* (kg/MMBTU)
$GWP_{g,c,s}$	Global Warming Potential caused by contaminant c from generator *g* in scenario *s* (1 kg CO_2 eq.)
$H_{g,seg}^{linear}$	Linearized Heat production of generator *g* in generation segment *seg* (MMBTU/MW)
$HTP_{g,c,s}$	Human Toxicity Potential caused by contaminant c from generator *g* in scenario *s* (1 kg toluene eq.)
i_k^{max}	Maximum number of D-FACTS that can be allocated per line.
I	Interest rate/discount rate.
l_{max}^{alloc}	Max. number of lines in which D-FACTS devices may be allocated
l_k	Length of line *k*
$L_{n,s}$	Load at bus *n* in scenario *s*.
N	Lifespan of D-FACTS devices.
N_c	Total number of contaminants considered
N_g	Total number of generators.
N_k	Total number of lines.
N_s	Number of scenarios.
N_{seg}	Number of segments for the linearized generator cost function.
N_{pop}	Population size for the algorithm.
N_r	Number of renewable generators.
p_s	Probability of scenario *s*.
P_g^{max}	Upper generation limit of generator *g*.
P_g^{min}	Lower generation limit of generator *g*.
$P_{r,s}$	Renewable power from renewable generator r in scenario s
S^D	Spinning down reserve requirement *g*.
S^U	Spinning up reserve requirement *g*.
T_c	Toxicity of contaminant *c*
X_k	The reactance of transmission line *k*.
X_k^{max}	Maximum reactance of line *k* if D-FACTS are installed on this line.
X_k^{min}	Minimum reactance of line *k* if D-FACTS are installed on this line.
W_c	GWP factor for contaminant *c* (1 kg CO_2 eq.)
η_C	The maximum adjustment percentage of the line's reactance in the capacitive mode that a single D-FACTS module (1 device/phase/mile) can achieve.
η_L	The maximum adjustment percentage of the line's reactance in the inductive mode that a single D-FACTS module (1 device/phase/mile) can achieve.
$\Delta\theta_k^{max}$	Max. value of bus voltage angle difference for stability in line *k*.
$\Delta\theta_k^{min}$	Min. value of bus voltage angle difference for stability in line *k*.

1. Introduction

ELECTRIC power generation accounts for one-seventh of human exposure to air pollutants such as fine particulate matter 2.5 ($PM_{2.5}$), sulfur dioxide, and nitrogen oxides, and at least 40 % of greenhouse-causing CO_2 emissions in recent years. Residents in low-income areas are more likely to be affected by air pollution, resulting in environmental equity issues [1]. Studies such as [2] show that organic and inorganic compounds produced by coal-powered plants create an elevated risk of cancer in nearby areas up to 50 miles away, and case studies have shown that replacing low-efficiency generators can reduce harmful emissions by over 60 % [3]. To reduce the environmental and health hazards, many countries set goals for emission reduction or clean energy integration. For example, the U.S. set a goal to reach net-zero emissions by 2050. Reaching such a goal requires not only wide deployment of clean generation but also building sufficient infrastructure, such as transmission networks, to integrate renewable energy [4]. Today, transmission congestion is one of the biggest issues in the North American electric transmission grid and the leading cause of renewable energy curtailment [5]. Transmission congestion occurs when transmission line capacity or transformer active power flow limits cannot meet the needs [6], and transmission expansion or upgrades are usually the first solutions being considered. However, such expansion or upgrades cannot solve the problem in a timely manner. In 2015 alone, $20.1 billion were invested in transmission system upgrades, but many independent systems operators still reported considerable congestion-related costs even after heavy spending on upgrades [7]. As transmission congestion issues persist, it has become necessary to find new approaches to mitigate this problem other than solely relying on transmission expansion or upgrades.

Other than transmission expansion and upgrades, some proposed solutions to congestion issues include energy storage [8], electric vehicle (EV) integration [9], and other strategies, including generator rescheduling, load shedding, distributed generation allocation, nodal pricing, etc. [10]. One of the most effective and promising approaches to address transmission congestion, though, is using variable-impedance series Flexible AC Transmission Systems (FACTS), which can be used to provide effective power flow control as part of smart transmission systems, improving the transfer capability of the transmission network and enabling a more sustainable and reliable power delivery network [11]. Distributed FACTS (D-FACTS) is a lightweight version of FACTS. They have the advantages of lower per-unit cost, improved reliability, and much smaller physical space requirements. They are built in a modular fashion and can be attached to a transmission conductor or installed on transmission towers. There are three main types of D-FACTS devices: Distributed Series Static Compensator (DSSC), Distributed Series Reactor (DSR), and Distributed Series Impedance (DSI). DSR and DSI work mainly by adjusting line impedance, while DSSC functions similarly to a phase shifter [12].

Different types of FACTS and D-FACTS devices have different functionalities in the power grid, such as reducing transmission congestion and operational costs [13], improving the overall stability of power grids, preventing line degradation and power outages, and facilitating renewable energy integration [14]. Studies such as [15] recommend the use of D-FACTS devices for effectively controlling power flows in systems with distributed generation sources, including non-dispatchable energy resources such as solar and wind energies. It has been repeatedly proven that both variable-impedance type FACTS and D-FACTS are effective for smart power flow control. D-FACTS devices, in particular, have the advantages of providing enhanced grid utilization, increased flexibility in power flow control, and increased security and reliability compared to traditional FACTS devices.

The topic of D-FACTS allocation is still a relatively new concept, with the technology proposed in 2005 as a cost-effective, low-footprint solution to traditional FACTS devices. Since then, various studies have been done on the viability and cost-effectiveness of D-FACTS devices, as well as their role in improving overall power quality [14]. Different optimization methods have been adopted for the optimal allocation of such devices. One such optimization method is graph theory, used by Ref. [16] to control line flows under the presence of changing generation and loads. Particle swarm optimization (PSO) is another optimization method for D-FACTS allocation, which is suitable for graphic-based problems [17]. For example [18], focused on minimizing voltage deviation and power losses, maximizing voltage stability, and optimizing load balancing using an enhanced bacteria foraging optimization based on the particle swarm optimization (PSO) algorithm. PSO methods have also been used by Ref. [19] to minimize power loss and voltage deviations by allocating various types of D-FACTS devices. However, these D-FACTS allocation algorithms do not consider the uncertainties caused by load variation and renewable generation. Mixed-integer linear programming with stochastic scenarios was used by Ref. [20], allowing for accurate D-FACTS optimal allocation and configuration in meshed networks with uncertainties. However, due to a large number of integer variables in the optimization problem, computational efficiency is still a challenge.

Despite a variety of optimization methods for D-FACTS allocation, the literature still comes short in solving the optimal allocation and configuration of variable-impedance type D-FACTS considering system uncertainties with high computational efficiency. The major challenge is

that such problems require us to solve mixed-integer programs with a large number of integer variables considering a large number of constraints. Another gap to be addressed is utilizing D-FACTS to reduce the environmental impact of energy systems. Since D-FACTS devices affect the power flow patterns in the transmission network, they can significantly change the emissions, including $PM_{2.5}$, sulfur dioxide, nitrogen oxides, and carbon dioxide, from the power system. These emissions have varied impacts on the environment, causing not only greenhouse effects but also hazards to human health. Although there is a recent work studying the impact of FACTS on carbon emissions [21], there is still a lack of work that considers how different emissions affect both the environment and human health in D-FACTS allocation and configuration.

To address the computational challenge, a preliminary evolutionary algorithm (EA) was proposed in the authors' previous work [22]. The model had a single objective of minimizing system operating costs and did not consider the impact of D-FACTS allocation on environmental impacts. Thus, this paper aims to address the above-mentioned gaps by customizing and fine-tuning the EA for a comprehensive, multi-objective D-FACTS optimization model that considers not only operating cost reduction but also environmental impacts.

The contributions of the paper are listed as follows.

1) This paper proposes a multi-objective optimization model to optimally allocate and configure D-FACTS in meshed transmission networks, minimizing not only power system operating costs but also the environmental and human health impacts of power systems. The environmental and human health impact metrics used in this study are global warming potential (GWP), a metric used to determine how much heat the emissions are capable of trapping [23], and human toxicity potential (HTP), which measures long-term health risks for humans associated with inhalation and skin exposure to harmful substances.
2) A custom-made, computationally efficient evolutionary algorithm is proposed in this study to solve the nonlinear, computationally challenging D-FACTS optimization problem, considering a complete set of power system operating constraints and uncertainties. The model can optimally allocate D-FACTS modules over the entire line instead of allocating the modules per mile, offering flexibility in the number of D-FACTS modules to be allocated for each line.
3) An analysis of the trade-off between power system operating costs, GWP, and HTP, with the use of D-FACTS, is presented in this paper. In the case studies, Pareto fronts were obtained using the proposed method. The Pareto fronts show inverse relationships between power system operating costs and the environmental and human health impacts, and decision-makers can choose a Pareto-optimal D-FACTS allocation and configuration solution based on their budget and environmental impact mitigation goals.

The remainder of this paper is organized as follows: Section II describes the mathematical formulation of the multi-objective D-FACTS optimization model, Section III presents the proposed evolutionary algorithm, Section IV presents case studies and analyzes the results, and conclusions are drawn in Section V.

2. D-FACTS optimization model formulation

The proposed multi-objective optimization model allocates D-FACTS modules in each phase with the objectives of minimizing power system operating costs, GWP, and HTP, respectively, while satisfying different power system operating constraints. The model also automatically configures D-FACTS modules with optimized set points. In the proposed model, D-FACTS modules are allocated along a number of transmission lines in a system. Since the reactances of the lines will be adjusted by the D-FACTS devices that will be installed, the equations describing power flow will change based on whether the flow is traveling in the reference direction (1) or against it (2) [24]:

If $\theta_{fr,k,s} - \theta_{to,k,s} \geq 0$,

$$\theta_{fr,k,s} - \theta_{to,k,s}/X_k^{max} \leq F_{k,s} \leq \theta_{fr,k,s} - \theta_{to,k,s}/X_k^{min} \tag{1}$$

If $\theta_{fr,k,s} - \theta_{to,k,s} \leq 0$,

$$\theta_{fr,k,s} - \theta_{to,k,s}/X_k^{min} \leq F_{k,s} \leq \theta_{fr,k,s} - \theta_{to,k,s}/X_k^{max} \tag{2}$$

The formulation of the proposed D-FACTS optimization model considering power flow directions is described by Equations (3)–(28).

Objectives:

$$\min OF_1 = \sum_{s=1}^{N_s} P_s \left(\sum_{g=1}^{N_g} \left(\sum_{seg=1}^{N_{seg}} C_{g,seg}^{linear} P_{g,s}^{seg} + C_g^U R_{g,s}^U + C_g^D R_{g,s}^D + C_g^{NL} \right) + \sum_{r=1}^{N_r} c_r P_{r,s}^C \right) + C_{inv}^D \tag{3}$$

$$\min \mathrm{OF}_2 = \left(\sum_{s=1}^{N_s} \left(P_s \sum_{g=1}^{N_g} \sum_{c=1}^{N_c} GWP_{g,c,s} \right) \right) \tag{4}$$

$$\min OF_3 = \left(\sum_{s=1}^{N_s} \left(P_s \sum_{g=1}^{N_g} \sum_{c=1}^{N_c} HTP_{g,c,s} \right) \right) \tag{5}$$

Constraints:

$$P_{g,s} = \sum_{seg=1}^{N_{seg}} P_{g,s}^{seg} \tag{6}$$

$$P_g^{min} \leq P_{g,s} \leq P_g^{max} \tag{7}$$

$$-F_k^{max} \leq F_{k,s} \leq F_k^{max} \tag{8}$$

$$\sum_{k \in \sigma^+(n)} F_{k,s} - \sum_{k \in \sigma^-(n)} F_{k,s} + \sum_{g \in g(n)} P_{g,s} + \sum_{r \in r(n)} \left(P_{r,s} - P_{r,s}^C \right) = L_{n,s} \tag{9}$$

$$\sum_{g=1}^{N_g} R_{g,s}^U \geq S^U \tag{10}$$

$$\sum_{g=1}^{N_g} R_{g,s}^D \geq S^D \tag{11}$$

$$R_{g,s}^U \leq P_g^{max} - P_{g,s} \tag{12}$$

$$R_{g,s}^D \leq P_{g,s} - P_g^{min} \tag{13}$$

$$R_{g,s}^U \geq 0 \tag{14}$$

$$R_{g,s}^D \geq 0 \tag{15}$$

$$\Delta\theta_k^{min} \leq \theta_{fr,k,s} - \theta_{to,k,s} \leq \Delta\theta_k^{max} \tag{16}$$

$$\theta_{1,s} = 0 \tag{17}$$

$$f_{k,s} \left(1 + \frac{x_k^D}{l_k} \eta_L \right) X_k F_{k,s} \geq f_{k,s} \left(\theta_{fr,k,s} - \theta_{to,k,s} \right) \tag{18}$$

$$f_{k,s} \left(1 + \frac{x_k^D}{l_k} \eta_C \right) X_k F_{k,s} \leq f_{k,s} \left(\theta_{fr,k,s} - \theta_{to,k,s} \right) \tag{19}$$

$$0 \leq x_k^D \leq i_k^{max} \tag{20}$$

$$\sum_{k=1}^{N_k} \frac{x_k^D}{\max(x_k^D, 1)} \leq l_{max}^{alloc} \tag{21}$$

$$GWP_{g,c,s} = \sum_{seg}^{N_{seg}} H_{g,seg}^{linear} P_{g,s}^{seg} G_{g,s} W_c \tag{22}$$

$$HTP_{g,c,s} = \sum_{seg}^{N_{seg}} H_{g,seg}^{linear} P_{g,s}^{seg} G_{g,s} T_c \tag{23}$$

$$C_{inv}^{D} = \sum_{k=1}^{N_k} 3C_{sh}^{D} x_k^{D} \tag{24}$$

$$C_{inv}^{D} \leq C_{inv}^{max} \tag{25}$$

$$C_{sh}^{D} = C_{single}^{D} \frac{I(1+I)^N}{8760\left((1+I)^N - 1\right)} \tag{26}$$

$$0 \leq P_{r,s}^{C} \leq P_{r,s} \tag{27}$$

$$\phi^{C} = \sum_{s=1}^{N_s} \sum_{r=1}^{N_r} \frac{P_{r,s}^{C} p_s}{P_{r,s}} \tag{28}$$

In this formulation, the objectives are to minimize the total power system operating costs, including generation and reserve costs as well as D-FACTS investment costs, as shown in Equation (3), and to minimize GWP and HTP, as shown in Equations (4) and (5), respectively. Equation (6) segments and linearizes the generation cost function, while (7) establishes the upper and lower generation limits for each generator in the system. Equation (8) sets the transmission limits for each line. The power balance at each bus in the system is defined by (9), which ensures that the load at each bus equals all the power generated at each bus plus the incoming line transfers minus the outgoing line transfers. Equations (10)–(15) define the spinning up and down reserve requirements, with (10) and (11) defining required total spinning up and down reserve capacities, (12) and (13) setting a limit on maximum reserve that could be scheduled from each generator, and (14) and (15) ensuring that the spinning up and down reserves are nonnegative. Equation (16) defines the voltage angle constraints, and (17) sets bus 1 as the reference bus. Furthermore, Equations (18) and (19) calculate the power flow on each line, considering possible D-FACTS installations on the lines. In these two equations, the power flow direction (f_k) can be either +1 or −1. The values of f_k are obtained by solving the model with no D-FACTS installed, in which $f_k = 1$ and $x_k^D = 0$. Equation (20) sets a limit on how many D-FACTS can be installed on each line, and Equation (21) limits the number of lines at which D-FACTS can be installed. Equation (22) calculates the GWP of each generator considering the pollutants it releases based on the piecewise linear heat-based emission curves. In this equation, the GWP factors are obtained from Ref. [23]. Equation (23) calculates the HTP of each generator in a similar way, using the HTP factors in Ref. [25]. Equation (24) calculates the total investment cost of D-FACTS, which is limited in (25) and converted into an hourly figure in (26), considering a discount rate and the expected lifespan of D-FACTS modules. Additionally, (27) defines the upper and lower bounds for renewable energy curtailment, while (28) defines the wind energy curtailment percentages.

Since the optimization problem is a nonlinear program, it is very computationally complex. But the metaheuristic approach proposed below in Section III removes the nonlinearities by pre-establishing the values of x_k^D and reduces the problem into a linear program that linear optimization solvers can solve.

3. The evolutionary algorithm

Metaheuristic search methods are steadily gaining traction in optimization research due to their quick convergence and low computational burden. They are able to achieve good near-optimal solutions by performing a quick, effective, and intelligent search of the solution space, and their can solve problems that cannot always be solved using traditional mathematical approaches [26].

This paper presents a custom-made MOEA which is fine-tuned to efficiently find possible solutions to the D-FACTS allocation problem and identify which of them meet optimality conditions. The MOEA was modified by separating the sub-problem that it solves into a generation dispatch problem, a linear program (LP) and a greedy reserve allocation problem to reduce the expected computational time from the simplex algorithm which runs on polynomial time. The reason to replace part of the problem with a greedy algorithm is that the greedy algorithm runs on linear time.

As this is a multiple-objective optimization problem, it is both possible and expected that at least some of the objectives are in opposition to each other, and that a single optimal solution cannot be determined without assistance from a decision-maker. For this type of situation, the Pareto optimality is considered. If no better solution can be found than a solution without sacrificing other objective values, then this solution is called a Pareto optimal solution. At the end of an optimization method that uses Pareto optimality, the result is a set of Pareto-optimal solutions called the Pareto front or Pareto-optimal set. This set of solutions can then be further analyzed in a procedure called post-Pareto optimality.

The proposed MOEA begins by generating sets of random values within the possible solution space. Each of these sets is called a chromosome, representing a possible solution to the problem. The chromosome is a 1-dimensional vector array, representing the number of D-FACTS devices to be installed in each line, based on the limits allowed by the maximum reactance adjustment allowed for each line and the adjustment range for each device, with the constraints defined in (20) and (21). Fig. 1 is a flowchart that shows the process adopted by the algorithm. At each iteration, a set of possible solutions, or population, is generated. At the first iteration, the population is generated randomly, while in subsequent iterations, it is generated based on the previous population by a process known as crossover, where two of the current generation's solutions will be chosen and combined to produce a new solution. After generating the population, each solution or chromosome is first employed in a reduced LP model, consisting of Equations (3)–(9), (16)–(19), (22), (23), (27), (28) which would minimize the total generation cost, GWP, and HTP in a single scenario at a time, giving priority to the cost function and then obtaining the related GWP and HTP based on the LP solution, while the reserves are assigned by a greedy algorithm based on the solution of the LP and Equations (10)–(15), before producing a weighted average of these costs using the scenario probabilities as weights and adding the D-FACTS cost given by (24). The dominance of each solution is checked via (29). Solutions that satisfy (30) are considered non-dominated and stored. After evaluating the objective functions for each solution, they need to be combined into a single value in order for the crossover function to operate properly. To do this, two fitness metrics are created, based on proximity to the true Pareto front and inter-solution distance, to ensure that the solutions generated are both closer to the true limits of the Pareto front and well spread over it [27]. These functions are then normalized and combined to produce a single aggregated fitness metric.

Proximity to the true Pareto front is not measurable as we do not have any information on it. However, we can establish that more dominant solutions must be closer to it. Thus, the first fitness metric is a dominance count for each solution. The dominance is defined in (29), stating that solution a dominates solution b if it is better than it in all objectives, and the associated fitness metric for dominance is defined in (31). This metric is shown in (32) as the sum of all inter-solution objective function distances, assuming they have been normalized to the (0,1) range. At the end, The aggregated fitness metric is then calculated by the formula given in (33).

$$If\ OF_{obj,a} \leq OF_{obj,b}\ \forall obj;\ \ D_{a,b} = 1;\ else, D_{a,b} = 0 \tag{29}$$

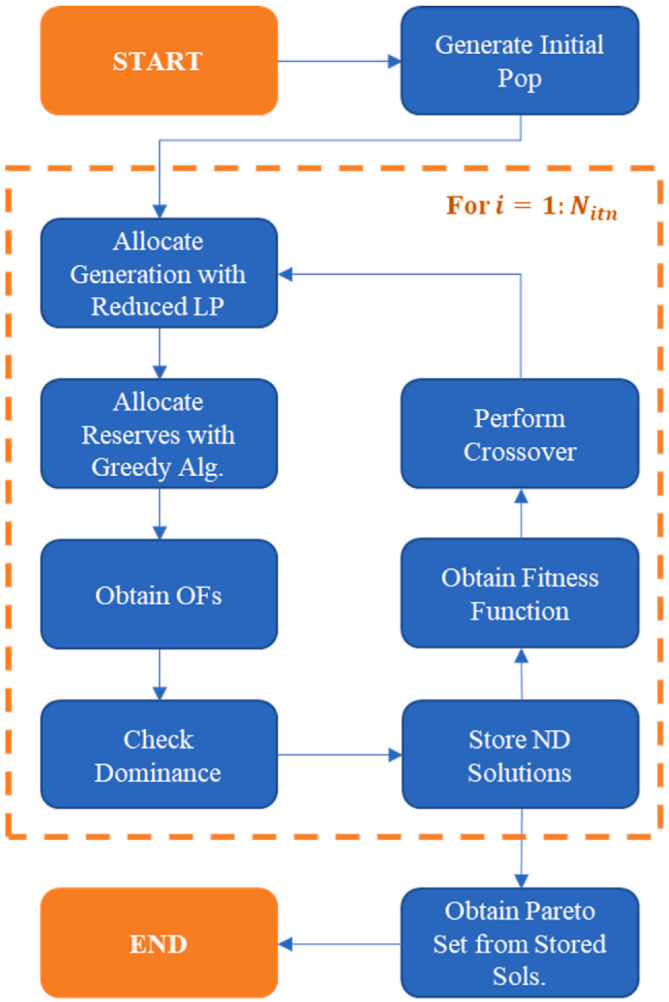

Fig. 1. Evolutionary algorithm flowchart.

$$\sum_{a=1}^{N_{pop}} D_{a,b} = 0 \tag{30}$$

$$FM_{1,a} = \sum_{b=1}^{N_{pop}} D_{a,b} \tag{31}$$

$$FM_{2,a} = \sum_{b=1}^{N_{pop}} \left[\sum_{obj=1}^{N_{obj}} \left(OF_{obj,a} - OF_{obj,b} \right)^2 \right]^{\frac{1}{2}} \tag{32}$$

$$FM_{0,a} = \frac{FM_{1,a}}{\max_b FM_{1,b}} + \frac{FM_{2,a}}{\max_b FM_{2,b}} \tag{33}$$

After calculating the aggregated fitness metric and ranking the solutions accordingly, a tournament-type selection is held to select the parents for each new solution. In this, four solutions are selected and paired. The solution with the better fitness metric is stored in each pair, and the remaining two are combined with a single cut-point, resulting in a new candidate solution. Two processes, one known as elitism and the other as mutation, are incorporated into the crossover process. Elitism guarantees good solutions in the new population while mutation helps avoid falling into local optima and increases solution diversity. Elitism automatically transfers a percentage of the previous population into the new one. Mutation works by randomly switching some of the values in a solution if a parameter falls within a threshold.

After all the iterations, dominance is checked again over the stored solutions in order to find the optimal Pareto set for the problem so that they may be presented to a decision-maker for final decision-making based on their specific needs.

4. Case studies

A Simulation Setup

For the simulation study, the model from Section II was adopted to study the cost-effectiveness and environmental benefits of D-FACTS, and it was solved using the algorithm proposed in Section III. The simulations were carried out on a modified IEEE RTS-96 test system. Modifications to the system were made to add congestion to the system, so that the system becomes suitable for analyzing the impact of D-FACTS implementations. These modifications are a shifting of 480 MW of load towards bus 13, and a reduction in the capacity rating in five of the lines in order to create congestion. The modifications were made based on a realistic cause of transmission congestion, namely, a lack of transmission capacity between load centers and generation sources. Similar modifications have been widely adopted in previous research on flexible transmission systems, such as References [5,13,20,21,28], and [29]. The original RTS-96 test system includes different types of generation sources, including oil-fired, coal-fired, hydroelectric and nuclear generators. Nuclear generators are usually used to serve the base load, while the oil-fired, coal-fired, hydroelectric generators are dispatchable generation sources. These generators are usually not considered as sources of uncertainties in power system operations. To study the impact of the uncertainties of renewable energy sources, we added two 400-MW wind farms on buses 19 and 20 of the system for the cases in which wind energy was considered. For the cases where solar energy was considered, a 200 MW solar farm was added to bus 22. Rooftop solar panels equating to 10 % of the load at the buses, rounded to the nearest 5 MW, were also added for the cases with solar energy, and the total rooftop solar generation capacity was 225 MW. Thus, a total solar capacity of 425 MW was considered in case studies with solar energy in this paper. The test system is shown in Fig. 2, where the locations for wind generators are marked with blue circles with "WT400" on them, the location of the solar farm is marked with a yellow parallelogram with "PV200" on it, and the locations of rooftop solar panels are marked with green rectangles with "RS" on them.

Uncertainties in this study are from two sources, namely, load and renewable energy generation. Renewable energy considered in this study includes solar and wind energy. Despite an abundance of different types of renewable energy sources, the two were selected because they have a high potential for future energy production. According to a technical report by the U.S. Department of Energy, solar and wind are the two renewable energy sources with the highest energy potential [30]. The two renewable energy sources are kept separate for two reasons. First, the availability of solar and wind energy is subject to climate conditions in different geographic regions. Research shows that regions with abundant solar and wind energy usually do not overlap [31,32]. Second, solar and wind energy sources have different characteristics, and thus have different impacts on power grid operations. It is paramount to study the patterns of impact by each source individually. As such, the following three cases were formulated in this study.

- **Case I:** Only the uncertainty of load is considered, and four different load scenarios with load factors at 0.65, 0.75, 0.85, and 0.95 are adopted as per [20]. These scenarios attempt to simulate possible load factors at different times of day.
- **Case II:** The uncertainties in both the load and wind energy generation are considered. Wind energy scenarios were introduced to the system with four different renewable energy scenarios at 0 %, 20 %, 60 %, and 100 % of the rated wind energy generation capacity. With a cross-product of the load and renewable generation scenarios, a total of 16 scenarios were created to represent the uncertainties.

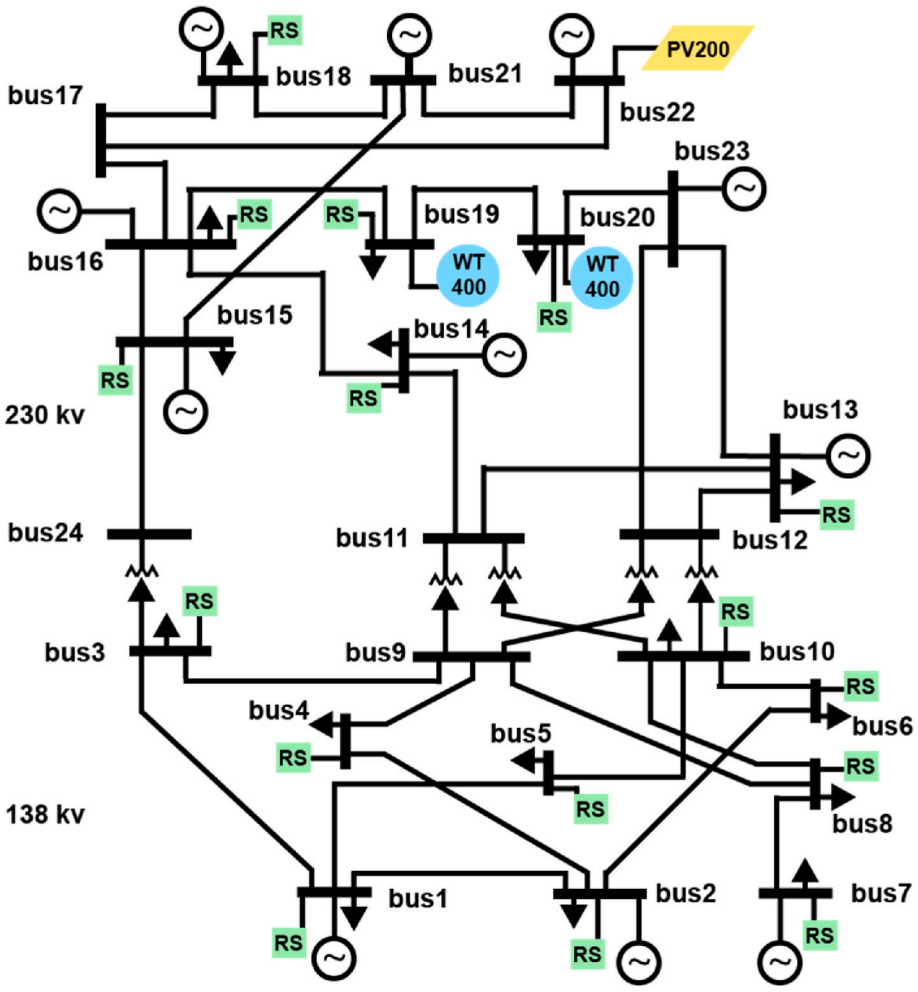

Fig. 2. The modified RTS-96 test system with added wind turbines (WT), photovoltaic farm (PV) and rooftop solar (RS) locations.

- **Case III:** The uncertainties in both load and solar generation are considered. Solar generation scenarios were created based on the NREL PVWatts Calculator for the city of El Paso. For simplicity, these scenarios were set at 0 %, 30 %, 50 %, and 85 % of the rated capacity for regular solar panels, with 0 % holding the highest probability as solar panels produce virtually no energy for half the day. Just as with Case II, there is a total of 16 scenarios in this case.

B D-FACTS Parameters

It is assumed that each D-FACTS module is designed to be able to adjust the line's reactance by ±2.5% per phase per mile, with a maximum reactance adjustment range for a 3-phase line of ± 20%. D-FACTS allocation results were obtained with the assumption that the modules are allocated evenly per line per phase. Given the devices' adjustment range and the line adjustment limits, the maximum number of devices allowed is estimated to be $20/2.5 = 8$ devices per mile for each line.

D-FACTS costs were determined based on industry data and previous academic studies [20], assuming the cost for a device of $100/kVA, where the compensation level in kVA depends on the parameters of the line in which the device is installed. For simplicity, the compensation level for the most demanding line was adopted. In the modified RTS-96 system, the largest compensation level is 30 kVA/module. Thus, a cost of $3000 per module is used for this study. The hourly cost of devices is obtained based on (26), with an assumed lifespan N of 30 years and a discount rate I of 6 % as in Ref. [20]. Equation (25) denotes the investment limit on the D-FACTS modules. For this study, a maximum allowance of $25/hour is assumed.

C Costs, GWP, HTP, and Wind Energy Curtailment

The MOEA was programmed on MATLAB® 2019a and run with the following parameters: 500 individuals over 100 iterations, with 10 % elitism and a 5 % chance of mutation. The algorithm was run on a Dell computer with 256 GB of RAM and an Intel® Xeon® W-2195 CPU. From the simulation results, we obtained power system operating costs, GWP, and HTP from each solution in the first two cases, and they are summarized in Fig. 3 for Case I and Fig. 4 for Case II. The figures show nonlinear relations between the objectives, indicating that attempting to reduce one of the objectives will result in an increase for the other ones, although this is not necessarily a linear relation. This is to be expected when looking at the generator data, as cheaper generators in the test system have much higher emission rates than the more expensive ones. However, this conflict exists mainly between the costs and environmental impact objectives rather than between the two environmental impact metrics. It is also noticeable that while there is some linearity in the trendline for Case I, there is none for Case II. This is due to the uncertainties associated with the inclusion of wind energy into the system which, depending on the power flow control settings and generator dispatch, can have a much larger effect on the system and the objectives being optimized.

Details regarding power system operating cost, GWP, HTP, and renewable energy curtailment (%) for Cases I – III are given in Table 1 for the non-dominated solutions in the Pareto front. The numbers of non-

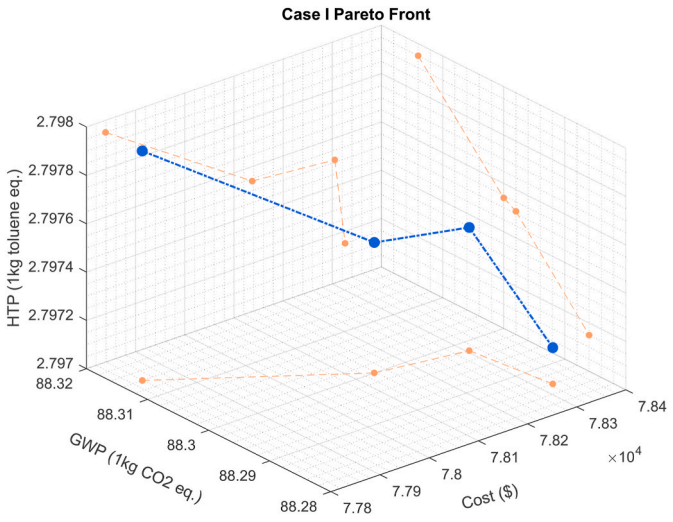

Fig. 3. Case I Pareto front.

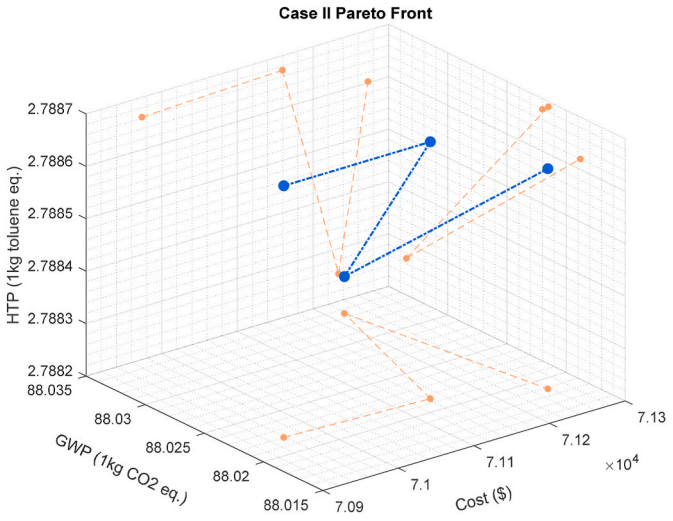

Fig. 4. Case II Pareto front.

Table 1
Details of selected solutions.

Case	#	Cost	GWP	HTP	Renewable Energy Curtailment
I	1a	77,839	88.314	2.798	N/A
I	1b	78,137	88.300	2.798	N/A
I	1c	78,305	88.298	2.797	N/A
I	1d	78,326	88.286	2.797	N/A
I	1e	79,494	88.320	2.800	N/A
II	2a	70,958	88.022	2.789	60.40 %
II	2b	71,144	88.021	2.789	61.31 %
II	2c	71,218	88.033	2.788	60.02 %
II	2d	71,257	88.019	2.789	60.22 %
II	2e	73,114	88.060	2.790	64.45 %
III	3a	68,743	54.2624	1.7195	51.76 %
III	3b	68,835	54.2403	1.7188	51.76 %
III	3c	69,651	54.2704	1.7198	51.76 %

dominant solutions differ depending on the cases; four non-dominated solutions were found in Cases I and II, respectively, and two non-dominated solutions were found in Case III. The solutions from Case I were numbered as 1a, 1b, 1c, and 1d, respectively, those from Case II were 2a, 2b, 2c, and 2d, respectively, and the ones from Case III were number 3a and 3b. We also ran a base case with no D-FACTS for each case and numbered them as 1e, 2e. and 3c, respectively. Base case 1e follows the conditions specified in Case I, base case 2e follows those in Case II, and base case 3c follows the conditions for Case III. This allows us to compare the system operating cost, GWP, and HTP in cases with and without D-FACTS. The unit of GWP in the table is 1 kg CO_2 eq., and the unit of HTP is 1 kg toluene eq.

As the table shows, under all the three cases, generation dispatch cost, GWP, and HTP are lower when using D-FACTS, compared to the base cases without D-FACTS. In all the three cases, there is a negative correlation between cost reduction and GWP, meaning that reducing generation dispatch cost is at the cost of increasing GWP. Without solar or wind energy, the GWP is mainly affected by the generation output of the coal and oil-fired generators. The energy production cost of coal-fired generators is much cheaper than that of oil-fired generators, but they have a higher carbon dioxide emission. Thus, when a preference is put on reducing cost, the GWP will increase. The sub-cases under Case II saw the most prominent reductions in generation dispatch costs and GWP, because the adoption of D-FACTS helped to reduce wind energy curtailment. Wind turbines have zero fuel costs and emissions during their operation, and an enhanced integration of wind energy helped to further reduce the generation dispatch costs and GWP. The generation dispatch cost and HTP, however, are not always negatively correlated. This is because coal-fired generators, although have a higher emission rate for carbon dioxide, do not have a high emission rate on all the gases that are hazardous to human health. Coal-fired generators have similar emission rates for nitrogen oxides as oil-fired generators, and lower emission rates for carbon monoxide and volatile organic compounds (VOCs) than oil-fired generators. The sub-cases in Case III saw the lowest generation dispatch cost, GWP, and HTP, compared to the cases with wind energy or without renewable energy, but they also saw the lowest reductions in generation dispatch cost, GWP, and HTP, mainly because solar energy has a distributed feature. Due to the widespread, distributed rooftop solar panels, the integration of solar energy is less affected by transmission constraints. Thus, solar energy tends to be better integrated than wind energy in a congested transmission network. Solar energy incurs zero fuel costs and emissions, and the better integrated solar energy helped to reduce the cost, GWP, and HTP overall. However, since the integration of solar energy is less affected by transmission constraints, mitigating transmission congestion does not enhance the integration of solar energy as effectively as that of wind energy, and this leads to lower reductions in costs, GWP, and HTP when using D-FACTS.

To further compare the results, the percentages of reduction in system operating cost, GWP, HTP, and renewable energy curtailment in the cases with D-FACTS compared to the ones without D-FACTS were calculated and presented in Table 2. It can be observed that D-FACTS could reduce system operating cost by up to 2.08 % in Case I, 2.95 % in Case II, and 1.30 % for Case III. D-FACTS could also reduce the GWP by up to 0.04 % in Case I, 0.05 % in Case II, and 0.06 % in Case III, and the HTP by up to 0.11 % in Case I, 0.07 % in Case II, and 0.06 % in Case III. Since the objectives of the optimization problem are minimizing costs, GWP, and HTP, the renewable energy curtailment may or may not be

Table 2
Reduction in costs and environment impact indices.

Case	#	Cost	GWP	HTP	Renewable Energy Curtailment
I	1a	2.08 %	0.01 %	0.07 %	N/A
I	1b	1.71 %	0.02 %	0.07 %	N/A
I	1c	1.50 %	0.02 %	0.11 %	N/A
I	1d	1.47 %	0.04 %	0.11 %	N/A
II	2a	2.95 %	0.04 %	0.04 %	6.28 %
II	2b	2.69 %	0.04 %	0.04 %	4.87 %
II	2c	2.59 %	0.03 %	0.07 %	6.87 %
II	2d	2.54 %	0.05 %	0.04 %	6.56 %
III	3a	1.30 %	0.01 %	0.02 %	0 %
III	3b	1.17 %	0.06 %	0.06 %	0 %

reduced. In this study, while the wind energy curtailment was improved in Case II by the D-FACTS, with a reduction of about 5–7% in the different cases, the curtailment of solar power did not change in Case III, mainly due to the distributed feature of solar energy, as analyzed in the previous paragraph.

The mild reductions in environmental impacts are due to the cost-oriented optimization coded into the algorithm, and power system operators tend to follow the same reasoning in their business decisions. If more priority were given to environmental impacts, it would be possible to further reduce GWP or HTP with the usage of D-FACTS. However, in this case, the operational costs may increase, which is not a desirable outcome for power system operators. Additionally, since power system operations cost hundreds of billions of dollars and produce an estimated 1.55 billion metric tons of CO_2 in the U.S. each year, even a small percentage of cost, GWP, and HTP reduction can result in significant economic, environmental, and health benefits in real-world power systems.

According to a 2023 report [33], the territory managed by the Electric Reliability Council of Texas (ERCOT) currently has a wind energy penetration of 27.3 %. Meanwhile, the wind energy penetration of the territory managed by the California Independent System Operator (CAISO) is 6.9 % as of 2022 [34]. By comparison, the test system used in this study has a wind penetration of 23.5 %, which is similar to the wind energy penetration level of the ERCOT grid and much higher than that of CAISO. The same sources list a solar penetration of 13.4 % for Texas and 19.9 % for California, compared to 12.5 % for our system. Based on the information for Texas, the state curtailed 5 % of its wind energy and 9 % of its solar energy in 2022. Although the curtailment percentage is small, the total capacity curtailed is significant due to the large scale of the system. Take the ERCOT power grid as an example, the system curtails around 2000 MWh renewable energy every hour on average. As the simulation results in this study show, D-FACTS can reduce renewable energy curtailment by above 5 % in many cases. If the 2000-MWh hourly curtailment can be reduced by 5 %, that means 100 MWh more renewable energy can be integrated into the system every hour.

D D-FACTS Allocation

The allocations of D-FACTS modules in the six representative solutions were obtained and presented in Table 3. All solutions except 1d (with 939) had a total of 999 devices installed. The maximum allowable number of D-FACTS modules is 999, based on the investment limits set in Equations (24)–(26). Although the quantities of D-FACTS modules allocated in the system were at their maximum in most cases, the number of D-FACTS modules allocated was smaller than the maximum in 1 out of the 8 solutions. This is because the optimization algorithm determined it served the objective best to use a specific number of D-FACTS modules considering all the factors, such as operating costs, GWP, HTP, and investment cost of D-FACTS that was converted into an hourly figure. The six solutions not only yielded different power system operating costs and GWPs, but also had D-FACTS modules allocated to different lines.

The test system has 38 transmission lines, and the D-FACTS modules were allocated on 2–5 lines in each solution. It can be seen from these solutions that some lines were more likely to be chosen as the location for D-FACTS installations. Lines 22 showed up in 8 out of the 10 solutions Line 28 showed up in 5 out of 10, Line 33 in 3 out of 10 solutions, and Lines 1, 4, 12, 24, 28 and 29 were chosen in 2 out of the 10 solutions. However, to ensure minimal values of system operating costs and impacts, each solution had a different combination of lines, and the lines could not be chosen individually. Thus, the optimization model can give us a better solution than using engineering judgments.

E D-FACTS Set Points

In addition to obtaining the Pareto-optimal allocation of the D-FACTS devices, we also calculated the set points for each line in which the devices were installed. The set point of the D-FACTS in a line refers to how much the devices adjusted the reactance of the line, as a percentage. The set points remained constant among the different scenarios for all solutions, and the set points are presented in Table 3.

Table 3
D-FACTS allocation of non-dominated solutions.

Case	#	Line Number	D-FACTS per line	Set Point
I	1a	1	9	−2.50 %
		22	990	13.79 %
I	1b	4	240	−6.06 %
		22	420	5.83 %
		28	285	13.19 %
		29	45	2.34 %
		37	9	0.50 %
I	1c	11	270	14.06 %
		22	291	4.04 %
		28	294	13.75 %
		30	144	12.00 %
I	1d	4	216	−5.45 %
		24	153	−10.63 %
		28	408	18.89 %
		33	162	7.50 %
II	2a	12	27	−0.52 %
		22	690	9.58 %
		24	108	−7.50 %
		37	174	9.67 %
II	2b	21	39	−0.49 %
		22	555	7.71 %
		28	165	7.64 %
		29	240	−12.50 %
II	2c	3	129	−4.89 %
		10	12	0.63 %
		13	57	1.10 %
		22	723	10.04 %
		36	78	4.33 %
II	2d	13	87	1.69 %
		20	225	−5.68 %
		22	639	8.88 %
		33	48	2.22 %
III	3a	1	9	−2.50 %
		22	990	13.79 %
III	3b	24	162	−11.25 %
		28	336	15.55 %
		33	189	8.75 %

It should be noted that while some lines, such as line 22, show up in most of the solutions, the set point for the line varies greatly between 4.04 % and 13.79 %. There are many factors that can account for this variability, from the number of devices allocated by the algorithm (more devices mean a larger adjustment range), to the variations in other lines helping control the power flow, which result in a different need to compensate the line. Line 22 is also a prime candidate for power flow control as it is connected to node 23, which is a generator node with a capacity for 760 MW and, depending on the generation dispatch, would be outputting a large amount of power through its attached lines, needing more adjustment for network transfer capability.

Overall, lines 11, 22, 28, and 30 were set at a high positive set point, while lines 4 and 24 had a high negative set point in Case I, while lines 22, 28, and 37 had high positive set points and lines 24 and 29 had high negative set points in Case II. In Case III, lines 22, 28, and 33 had high positive set points, while line 24 had a high negative set point. The other lines had some adjustments in their reactance, but the values were relatively close to 0, and this is largely due to the lower number of devices installed in those lines. Fig. 5, which shows the relationship between the number of devices installed in a line and the corresponding set points, indicates that some of the lines still have some slack in their adjustment capability, with the at-max devices following the straight

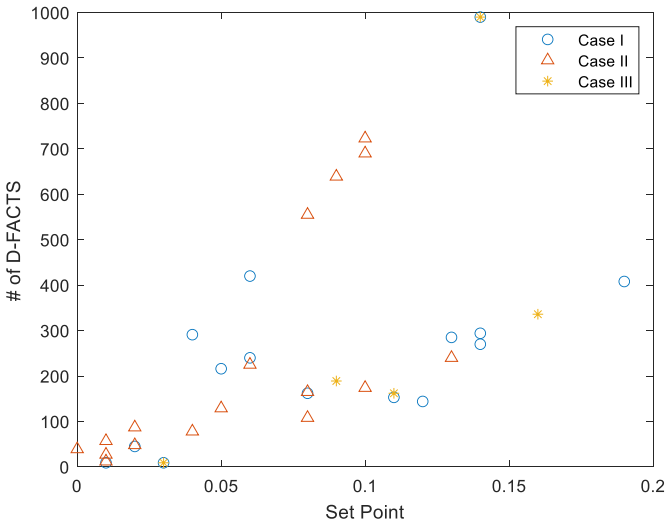

Fig. 5. Number of D-FACTS devices in a line vs. Setpoint (absolute value).

line at the top diagonal of the graph and the rest of the lines with some slack in their D-FACTS closer to the bottom.

F Computational Complexity

In the case studies, Case I was solved in 53.51 s, and Case II was solved in 55.23 s. As a comparison, the MILP with a similar formulation proposed by Ref. [8] had a computational time of 804.50 s on the same computer. The implementation of this evolutionary algorithm was capable of reducing the computational time by more than 90 %. This reduction in computational time can be a significant advantage over simplex method-based linear program solvers, especially when applied to large-scale transmission networks. Because of the order of magnitude for the number of operations for a linear model ($O(2^n)$ at worst) using the simplex method, D-FACTS optimal allocation problems can become computationally intractable using purely the simplex method. The method proposed in this study, while still relying partially on the simplex method, uses various strategies to reduce both the number of variables and constraints going into the simplex solver in order to largely mitigate the computational time requirements: first, the reserve requirements are extrapolated to a greedy heuristic, which runs in linear time. Second, the D-FACTS allocation is done by the metaheuristic, and thus it becomes possible to run the linear program (LP) for all scenarios separately. Effectively, it is much faster to run s instances of an LP with n variables than it is to run a single LP with $n{\cdot}s$ variables, since the runtime for the simplex method is at worst $O(2^n)$ and $s{\cdot}O(2^n) \ll O(2^{ns})$.

G Investment Cost and Return of D-FACTS

Since D-FACTS has an investment cost, it is important to study what is a reasonable investment level and how fast the investment can be recovered. Thus, we performed a sensitivity study in Cases I and II by varying the hourly investment limit C_{inv}^{max} in increments of $5/hour to best demonstrate the effects this has on the objective values and analyze the return of the investment. To demonstrate potential improvements on each of the objectives, this sensitivity study will not show the results from all non-dominated solutions at each investment level but the best objective function value at each. This way, it is possible to understand how much each objective function can be reduced by increasing the hourly investment limit.

Figs. 6–9 below show the change in the different objectives as the investment limit changes from $5/hour to $55/hour. These investment levels are hourly figures considering the lifespan of D-FACTS and a discount rate, as Equations (24)–(26) show. In Fig. 6, a clear downtrend

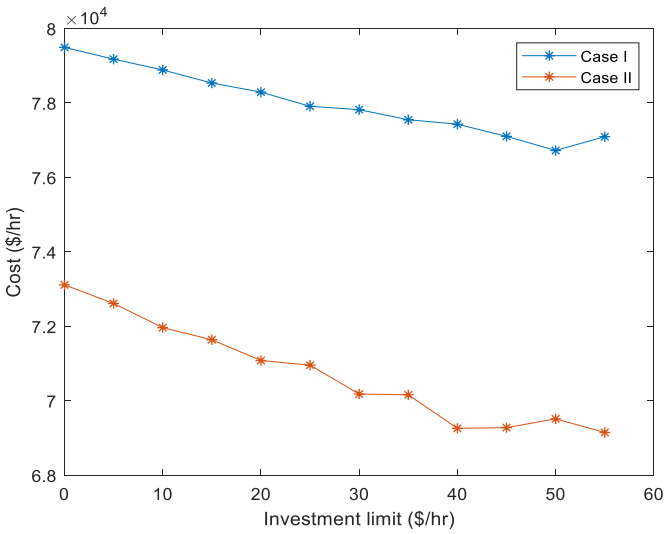

Fig. 6. Cost sensitivity analysis over investment limit.

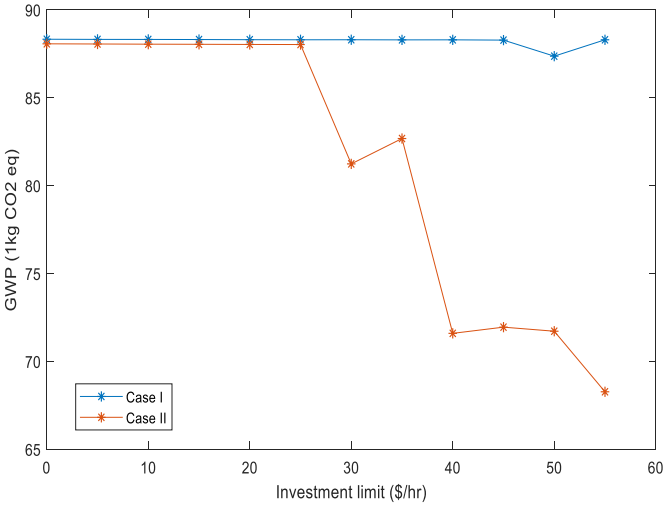

Fig. 7. GWP sensitivity analysis over investment limit.

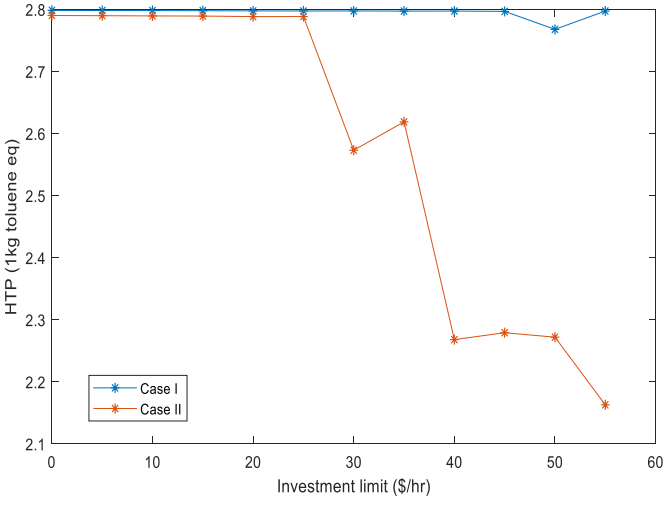

Fig. 8. HTP sensitivity analysis over investment limit.

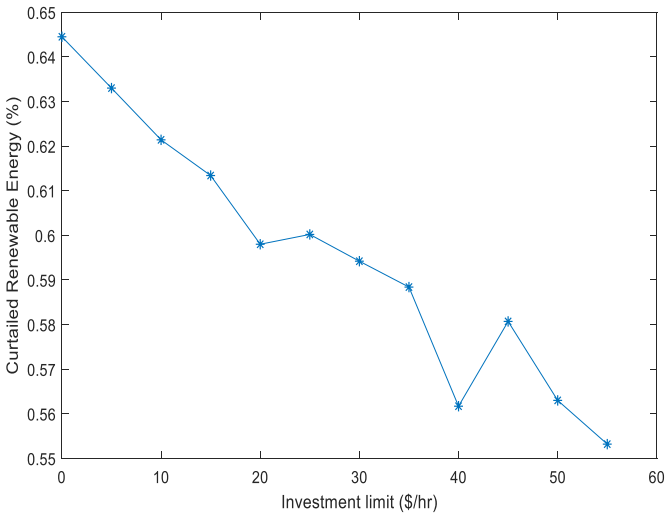

Fig. 9. Renewable energy curtailment sensitivity analysis over investment limit (Case II only).

can be seen in cost for both cases as the investment limit increases, so do GWP and HTP, as Figs. 7 and 8 show. However, this tapers off towards the right side of the graph as other constraints start tightening and there is less effect on the network. The limit on the number of lines over which the devices may be installed also plays a part on this tapering off the cost reductions.

For case II, however, the reduction in operating costs, GWP, and HTP is more obvious with the increase of D-FACTS investment, as more energy from the wind generators can be integrated into the system (shown in Fig. 9) and thus actual network emissions can be reduced enough for the environmental impact reductions to become more noticeable.

In this study, we assume a cost of $3000 per device and a 30-year lifespan. Each device accounts for approximately 2.5 cents/hour when converted to an hourly value. An hourly increase of only $5 translates to $602,900 in initial costs. Although there is a strong aversion to large investments with a long-term return, the savings in operating costs can be accrued very quickly. At the $25/hour limit, the investment is recovered in 1904 h in the case without wind energy, and in just 1399 h with wind energy, with the D-FACTS deployment solutions that minimize operating costs. This translates to 80 and 59 days, respectively. At an investment limit of $50/hr., it takes 2177 h and 1676 h to recover the investment, respectively, which are 91 and 70 days, respectively. These are still extremely short periods, after which the cost benefits grow exponentially, and the environmental and human health impact can be greatly mitigated. The analysis of the benefits of deploying D-FACTS devices in power grids can be used by utility companies to facilitate their decision-making in transmission planning.

5. Conclusions and future work

This paper proposes a multiple-objective evolutionary algorithm for solving optimal D-FACTS allocation and configuration problems. This algorithm has high computational efficiency and can optimally allocate a budgeted number of D-FACTS devices in electric power transmission systems considering power system operating costs, D-FACTS investment cost, GWP and HTP of the power system, as well as the uncertainties of load and renewable energy generation. The model was implemented on a modified RTS-96 test system, and the results show that optimally allocated D-FACTS can mitigate transmission congestion, reduce power system operating costs, and facilitate the integration of renewable energy, which can result in a significant reduction in environmental and human health impacts from the energy sector. The results also show that there is an inverse relation between the system operating cost and the two environmental impact metrics, GWP and HTP. A reduction in operating costs would generally increase environmental impacts, and vice versa. In each solution, the quantities and optimal locations, and set points for D-FACTS modules are very different from the others. In addition, a sensitivity analysis was performed in order to demonstrate the impacts of D-FACTS investment levels on power system operating costs, GWP and HTP. The results show that a high investment level of D-FACTS can result in more reduction in power system operating costs, GWP, and HTP, especially for power systems with a high penetration of renewable energy. The optimization model can provide decision-makers with a critical tool to determine where D-FACTS modules could be installed according to their budget, goals for environmental impact reduction, renewable energy integration, and access to transmission lines.

In future work, we plan to analyze the implementation of D-FACTS to facilitate the integration of mixed renewable energy resources with increased uncertainties. Additionally, we would like to consider different levels of renewable energy penetration in the system, considering the increasing popularity of renewable generation. Finally, we plan on looking into other solution methods which may further improve computational efficiency, such as machine learning.

CRediT authorship contribution statement

Eduardo J. Castillo Fatule: Writing – original draft, Visualization, Validation, Software, Methodology, Investigation, Formal analysis, Data curation. **Yuanrui Sang:** Writing – review & editing, Supervision, Software, Project administration, Methodology, Funding acquisition, Data curation, Conceptualization. **Jose F. Espiritu:** Writing – review & editing, Supervision, Project administration, Methodology.

Declaration of competing interest

The authors declare that they have no known competing financial interests or personal relationships that could have appeared to influence the work reported in this paper.

Acknowledgement

E. J. Castillo Fatule and Y. Sang's contributions to this work were supported by the U.S. National Science Foundation under Award #2131201.

Data availability

No data was used for the research described in the article.

References

[1] Tong D, Geng G, Zhang Q, Cheng J, Qin X, Hong C, He K, Davis SJ. Health co-benefits of climate change mitigation depend on strategic power plant retirements and pollution controls. Nat Clim Change 2021:1077–83.
[2] Artun GK, Polat N, Yay OD, Üzmez ÖÖ, Arı A, Tuygun GT, Elbir T, Altuğ H, Dumanoğlu Y, Döğeroğlu T, Dawood A, Odabasi M, Gaga EO. An integrative approach for determination of air pollution and its health effects in a coal fired power plant area by passive sampling. Atmos Environ 2017;150:331–45.
[3] Wu R, Liu F, Tong D, Zheng Y, Lei Y, Hong C, Li M, Liu J, Zheng B, Bo Y, Chen X, Li X, Zhang Q. Air quality and health benefits of China's emission control policies on coal-fired power plants during 2005–2020. Environ Res Lett 2019;14(9).
[4] U.S. Department of Energy's Office of Policy. On the path to 100% clean electricity. U.S. Department of Energy; May 2023.
[5] Sang Y, Sahraei-Ardakani M, Parvania M. Stochastic transmission impedance control for enhanced wind energy integration. IEEE Trans Sustain Energy 2017;9 (3):1108–17.
[6] Zhu L, Xu J, Yan L. Research on congestion elimination method of circuit overload and transmission congestion in the internet of things. Multimed Tool Appl 2017;76: 18047–66.
[7] Edison Electric Institute. Transmission projects: at a glance [Online]. Available: http://www.eei.org/issuesandpolicy/transmission/Documents/Trans_Project_lowres_bookmarked.pdf, ; 2016.

[8] Hemmati R, Saboori H, Jirdehi M. Stochastic planning and scheduling of energy storage systems for congestion management in electric power systems including renewable energy resources. Energy 2017;133:280–387.
[9] Nikoobakht A, Aghaei J, Mokarram MJ, Shafie-khah M, Catalão JP. Adaptive robust co-optimization of wind energy generation, electric vehicle batteries and flexible AC transmission system devices. Energy 2021;230.
[10] Yusoff NI, Zin AAM, Khairuddin AB. Congestion management in power system: a review. In: 2017 3rd international conference on power generation systems and renewable energy technologies (PGSRET); 2017.
[11] Mohandes B, El Moursi MS, Hatziargyriou N, El Khatib S. A review of power system flexibility with high penetration of renewables. IEEE Trans Power Syst 2019;34(4):3140–55.
[12] Johal H, Divan D. Design considerations for series-connected distributed FACTS converters. IEEE Trans Ind Appl 2007;43(6):1609–18.
[13] Sang Y, Sahraei-Ardakani M. Economic benefit comparison of D-FACTS and FACTS in transmission networks with uncertainties. In: 2018 IEEE power & energy society general meeting (PESGM); 2018.
[14] Gandoman FH, Ahmadi A, Sharaf AM, Siano P, Pou J, Hredzak B, Agelidis VG. Review of FACTS technologies and applications for power quality in smart grids with renewable energy systems. Renew Sustain Energy Rev 2018;82. 502-214.
[15] Muttaqi KM, Aghaei J, Ganapathy V, Nezhad AE. Technical challenges for electric power industries with implementation of distribution system automation in smart grids. Renew Sustain Energy Rev 2015;46:129–42.
[16] Mehta D, Ravindran A, Joshi B, Kamalasadan S. Graph theory based online optimal power flow control of Power Grid with distributed Flexible AC Transmission Systems (D-FACTS) Devices. In: 2015 North American power symposium (NAPS); 2015.
[17] Jordehi AR. Particle swarm optimisation (PSO) for allocation of FACTS devices in electric transmission systems: a review. Renew Sustain Energy Rev 2015;52:1260–7.
[18] Mohammadi M, Montazeri M, Abasi S. Bacterial graphical user interface oriented by particle swarm optimization strategy for optimization of multiple type DFACTS for power quality enhancement in distribution system. J Cent S Univ 2017;24:569–88.
[19] Zanganeh M, Moghaddam MS, Azarfar A, Vahedi M, Salehi N. Multi-area distribution grids optimization using D-FACTS devices by M-PSO algorithm. Energy Rep 2023;9:133–47.
[20] Sang Y, Sahraei-Ardakani M. Effective power flow control via distributed FACTS considering future uncertainties. Elec Power Syst Res 2019:127–36.
[21] Mirzapour O, Rui X, Sahraei-Ardakani M. Transmission impedance control impacts on carbon emissions and renewable energy curtailment. Energy 2023;278:127741.
[22] Castillo Fatule EJ, Espiritu JF, Taboada H, Sang Y. A computationally efficient evolutionary algorithm for stochastic D-FACTS optimization. In: 52nd North American power symposium (NAPS); 2020.
[23] US Environmental Protection Agency. Understanding global warming potentials [Online]. Available: https://www.epa.gov/ghgemissions/understanding-global-warming-potentials, . [Accessed 6 June 2023].
[24] Sahraei-Ardakani M, Hedman KW. A fast LP approach for enhanced utilization of variable impedance based FACTS devices. IEEE Trans Power Syst 2015;31(3):2204–13.
[25] Myhre G, Shindell D, Pongratz J. Anthropogenic and natural radiative forcing. In: Climate change 2013 : the physical science basis. Cambridge: Cambridge University Press; 2014. p. 659–740.
[26] Cheng JR, Gen M. Accelerating genetic algorithms with GPU computing: a selective overview. Computer & Industrial Engineering 2019;128:514–25.
[27] Fernandez JV. Development of post-Pareto optimality methods for multiple objective optimization. El Paso: The University of Texas at El Paso; 2017.
[28] Hedman KW, O'Neill RP, Fisher EB, Oren SS. Optimal transmission switching with contingency analysis. IEEE Trans Power Syst 2009;24(3):1577–86.
[29] Hedman KW, Ferris MC, O'Neill RP, Fisher EB, Oren SS. Co-optimization of generation unit commitment and transmission switching with N-1 reliability. IEEE Trans Power Syst 2010;25(2):1052–63.
[30] Brooks A. Renewable energy resource assessment information for the United States. Washington D.C.: U.S. Department of Energy; 2022.
[31] Draxl C, Hodge B, Clifton A, McCaa J. The wind integration national dataset (WIND) toolkit. Appl Energy 2015;151(8):355–66.
[32] Sengupta M, Xie Y, Lopez A, Habte A, Maclaurin G, Shelby J. The national solar radiation data base (NSRDB). Renew Sustain Energy Rev 2018;89(6):51–60.
[33] Hegar G. Wind power: energy is good for Texas. Texas Comptroller; 2023 [Online]. Available: https://comptroller.texas.gov/economy/economic-data/energy/2023/wind.php. [Accessed 9 January 2024].
[34] Nyberg M. Total system electric generation. California Energy Commission, 2023; 2022 [Online]. Available: https://www.energy.ca.gov/data-reports/energy-almanac/california-electricity-data/2022-total-system-electric-generation. [Accessed 9 January 2024].